Eng. & Tech. Journal, Vol.. 28 , No.17 , 2010

Experimental and Theoretical Investigation of Micro Pin Fins Heat Exchanger Used in Convective Cooling Application

Dr. Kutaeba J. AL-Khishali*, Dr. Mohammed I. Abu-Tabikh* & Auday.A.Abbo**

Received on: 3/6/2009
Accepted on: 11/3/2010

Abstract

Experimental and theoretical investigations of flow and thermal performance of an annular pin fin heat exchangers exposed to constant heat flux have been preformed. A special test rig was designed and built for this purpose. The main test section is an annulus of radius ratio (0.85) containing 10 rows of 1mm diameter pins with 5 pins in each row. The range of cooling air Reynolds number based on the hydraulic diameter of the channel, is (6774 to 11120). In the Theoretical part the well known Fluent (6.3) package was used for solving the governing equations for flow and Energy equation for heat transfer with RNG k-ε turbulence model. Results showed that the pin fins enhanced the heat transfer by a factor of (1.31 to 1.42) and increased the friction factor by (3 to 4) times compared to the one obtained for smooth annular channel without pins. A Nusselt-Reynolds correlation was obtained from the experimental data valid in the Reynolds number range studied. Reasonable agreement between the experimental and theoretical results was obtained with average difference (5%) over the Reynolds number range. The overall thermal performance obtained was larger than (1).

Keywords: Micro heat exchanger, Convective cooling, Pin fins

دراسة عملية ونظرية لمبادل حراري صغير ذو زعانف أبرية يستخدم في تطبيقات التبريد بالحمل

الخلاصة

تمت دراسة الجريان وانتقال الحرارة عمليا و نظريا في مبادل حراري حلقي ذو زعانف أبرية معرض إلى فيض حراري ثابت. تم تصميم وتنفيذ جهاز مختبري متكامل لهذا الغرض يتضمن مقطع اختبار على شكل قناة حلقية ذات نسبة أنصاف أقطار (0.85) تحتوي على 10 صفوف من زعانف أبرية بقطر1mm مرتبة بواقع 5 زعانف في كل صف. عدد رينولدز لهواء التبريد تراوح ضمن المدى (6700 إلى 11120). تم استخدام تقنية برمجيات FLUENT(6.3) لحل المعادلات الحاكمة للجريان وانتقال الحرارة مع استخدام نموذج الاضطراب (RNG k-ε). أظهرت النتائج أن

* Mechanical Engineering Department, University of Technology/ Baghdad
** MOE, Al –Taji Power Station/Baghdad

الزعانف الابرية تحسن من انتقال الحرارة بواقع (1.31 إلى 1.42) وتزيد من معامل الاحتكاك (3 إلى 4) مرات بالمقارنة مع قناة حلقية ملساء بدون زعانف. تم الوصول إلى معادلة تجريبية تربط عدد ناسلت مع عدد رينولدز نافذة المفعول ضمن مدى عدد رينولدز المحدد في التجارب. وتم الوصول إلى توافق معقول بين النتائج النظرية والعملية بمعدل فارق بين الاثنين بنسبة (5%). معامل الأداء الحراري الكلي للمبادل كان اكبر من (1).

Nomenclature

A	=Area	m^2	R	=Universal gas constant	J/kg.mol.K
Cp	=Specific heat	J/kg.K	S	=Span wise length	mm
D	=Cylinder diameter	mm	T	=Temperature	K
d	=Pin diameter	mm	V	=Velocity	m/s
f	=Friction factor	-	X	=Stream wise length	mm
h	=Convection heat transfer	$W/m^2.K$	η	=Efficiency	-
i	=Enthalpy	J/kg	μ	=Dynamic viscosity	kg/m.s
k	=Thermal conductivity	W/m.k	ρ	=Density	kg/m^3
L	=Length of test section	mm		**Subscripts**	
$\dot{m}$	=Mass flow rate	kg/s	b	=Bulk	
Nu	=Nusselt number	-	c	=Coolant	
P	=Pressure	N/m^2	f	=Film	
Pr	=Prandtl number	-	HE	=For heat exchanger	
Q	=Total heat	W	i	=Inner	
Re	=Reynolds number	-	**o**	=Outer	
r	=Radius	mm	w	=Wall	

1-Introduction

Pin fin micro heat exchangers have many applications such as cooling of power microelectronic, airframe structures, gas turbine blades, mechanical seals and many other applications in the biomechanical, automotive and aerospace industries. These heat exchangers are characterized by a very high heat transfer coefficient and could be adopted as alternatives to current cooling techniques in use today for gas turbine blades. The high heat removal from the blade surface will minimize the amount of air that have to be bled from the compressor to cool the turbine blades and hence increase the efficiency of the

gas turbine engine. In addition, it will provide a uniform temperature distribution that is needed to minimize the thermal stresses which increases the blade life span [1].

Numerous investigations have been carried out on macro-pin fin heat exchangers. Metzger et al. [2, 3] investigated the effects of the shapes, dimensions, and arrangement of pins on heat transfer coefficient and pressure drop in rectangular ducts while Chyu [4] and Chyu et al. [5] conducted studies on the effects of the operational surroundings on pin-fins, including end wall fillets and gaps at the top of the pin-arrays. Uzol and Camci [6], and Yan et al. [7,8] investigated the effect of pin shapes on heat transfer and pressure drops. Micro-pin fin heat exchangers seem to attract less attention. Mizunuma et al. [9] reported experimental and numerical results of forced convective heat transfer from a micro-finned surface. It was concluded that the increased flow velocity in the free flow area above the fins in higher height channels yield high heat transfer coefficients. Marques and Kelly [10] reported heat transfer and pressure drop results for flat parallel plate and curved pin fin micro heat exchangers with a staggered arrangement with application to gas turbine blade cooling. They found that the micro pin fin heat exchanger performance was better than a parallel plate counterpart.

The k–ε turbulence model is the most commonly used model for prediction of thermal and hydrodynamic characteristics of pin-fin micro-heat exchangers. Recently Galvis, et al. [11] examined several turbulence models using three dimensional finite element method for MHE (Micro Heat Exchanger) and compared their results with the experimental data of Metzger et al. [3]. They found that the RNG model (Renormalization Group Method) tended to be the best model to both the Nusselt number and the friction factor and captured the main features of the flow field in MHE. In the current study, experimental and theoretical investigations of fully-developed flow and thermal performance have been performed for a micro annular pin fin heat exchanger exposed to constant heat flux. The chosen flow conditions simulate those taking place at many convective cooling applications like the cooling of gas turbine blades.

2-Experimental Apparatus and procedures

Figure (1) shows schematically the basic components of the experimental test rig.

Main Test Section

The main test section is an annular channel of (110 mm long) fabricated from steel pipe of a thermal conductivity of 54W/m.K [12]. The inside and outside diameters are 23mm and 27 mm, respectively as shown in figure (2a). The outer cylinder has extensions of 15 mm from each end to provide threads for connection with inlet and outlet channels. The annular channel contains 10 rows of 1mm diameter steel pins with 5 pins in each row and height to diameter ratio equal to 2. The pedestal spacing varies from $S_o/d=17.2$ at the outer surface to

S_i/d=14.4 at inner surface of the annulus channel. An air pressure test was performed on the main test section alone to insure the tightness of the annulus by applying a pressure of 6 bars in de-ionized water pool. The arrangement of pins is a staggered and the grid distribution is shown in figure (3). Five holes 1 mm depth were drilled between the pins at upper surface and one hole at the middle of the lower surface for thermocouple junctions. Another smooth channel configuration (without pins) is fabricated with the same dimensions and used in the experiments for comparison.

To obtain a fully developed flow at the main test section inlet, an annular channel with length of 105 mm is added upstream of the main test section as shown in figure (2b). The channel made from tephlone PTFE (Poly Tetra Fluoro Ethylene) heat resistance plastic material. Also, the exit effect is minimized by adding 65 mm long annulus channel made of the same previous material as a downstream of the main test section, inlet and outlet channels are connected to the inlet and outlet reservoirs and the main test section is insulated by 5mm thickness fiber glass to reduce the heat transfer loss to the surrounding. Two holes are used for fitting the pressure transducers located at 13 mm up and down streams from the main test section.

Heating System

The heating system consists of two main tape heaters of 53mm length. The total power of the main heater is (200 W at 220 V). The heat flux is limited by an AVR (Automatic Voltage Regulator). A Guard heater of 100 mm length is also used to maintain a constant heat flux on the outer surface of the main test section. The control of this heater is also limited by the AVR. Two thermocouple junctions are located between the fiber glass insulation (50 mm in thickness) and tape guard heater. The heat input of the guard heater increased gradually in order to increase temperature and reaching a differences of 0.5^oC higher than temperature before starting and the AVR (Q_{loss}=0).

Measuring Techniques

An anemometer made by (H&M) Model Am- 4206 with accuracy ±0.2% was used for measuring the flow rate and it was fitted to the rig test by a suitable flanged joint. Inlet and outlet pressures in the test section (points P_{22} and P_{33}) are measured by a transducer type k100.The pressures in the inlet and outlet reservoirs (P_1 and P_4) are measured by Bourdon type pressure gauges. The Thermocouples of type k (Chromel positive, Alomel negative with temperature range -200C^o to 1300C^o) are used to measure temperatures. A digital electronic thermometer type (TM-914c) is connected to the thermocouples through a selector switch. The error of calibration during the test was not accesed 0.4 ^oC as compared with direct reading. The pressure and temperature measurement points are shown in figure (4)

Experimental Procedure

1- The air compressors are operated until the pressure reaches to the desired value (8 bar).

2- The chilled air dryer is started to reach the desired cooling air temperature (10 ^{o}C).
3- The main valve is opened and checking all gauges pressure readings.
4- The regulator valve is adjusted to the desired flow rate.
5- The heating system is operated for the main test section and adjusted by means of AVR.
6- The time of (25-35) minutes are allowed for the rig to reach a steady state.
7- The (flow rate, pressures, temperatures) measurements are performed.
8- Steps (4-7) are repeated for a new value of flow rate.
9- The procedure is repeated for the smooth channel configuration (without pins).

3-Analysis of Experimental Data

The properties of the coolant are evaluated at the film temperature T_f which is defined as:

$$T_f = \frac{T_w + T_b}{2} \qquad ....(1)$$

Where T_w is the average wall temperature and T_b is the bulk temperature of the coolant and is calculated by this equation:

$$T_b = \frac{T_2 + T_{3tot}}{2} \qquad .....(2)$$

T_2 and T_{3tot} are the static temperature at the inlet and the coolant total temperature at outlet of the heat exchanger, respectively. T_{3tot} is defined as the sum of the static temperature T_3 at outlet of the heat exchanger and the dynamic temperature change through the heat exchanger as written in equation (3) [1].

$$T_{3tot} = T_3 + \frac{1}{2Cp}(V_3^2 - V_2^2) \qquad .....(3)$$

The Choice of T_{3tot} instead of T_3 for calculation of T_b, can be explained by the fact that the heat exchangers transfer energy into the coolant not only in the form of internal energy but also in the form of kinetic energy [1].

The values of T_2 and T_3 are determined indirectly as follows[13], T_2 is the inlet temperature of the coolant and by applying the first law of thermodynamic at steady state condition between locations 1 &2 where m and i are the flow rate and the enthalpy of the coolant.

$$\dot{m}\left[(i_2 - i_1) + \frac{1}{2}(V_2^2 - V_1^2)\right] = 0 \qquad .....(4)$$

Using the assumption that air is an ideal gas, then:

$$i_2 - i_1 = Cp(T_2 - T_1) \qquad ..... (5)$$

And,

$$V_2 = \frac{\dot{m} RT_2}{A_2 P_2} \qquad .....(6)$$

Velocity V_2 is much larger than V_1 because the cross sectionarea of A_1 is a relatively large compared to A_2.

Combining equations (4,5,6) and solving for T_2 yield equation (7):

$$T_2 = \frac{-2Cp + \sqrt{(2.Cp)^2 - 4.(\frac{m.R}{A_2 P_2})^2.(-2.CpT_1)}}{2.(\frac{m.R}{A_2 P_2})^2} \quad -----7$$

Using the same steps above between locations 3 and 4 yields equation (8):

$$T_3 = \frac{-2Cp + \sqrt{(2.Cp)^2 - 4.(\frac{m.R}{A_3 P_3})^2.(-2.CpT_4)}}{2.(\frac{m.R}{A_3 P_3})^2} \quad ----8$$

Where

$$P_2 = P_{22} - \Delta P_{inlet}$$
$$P_3 = P_{33} + \Delta P_{exit}$$

ΔP_{inlet} and ΔP_{exit} is the pressure drop associated with the friction losses in inlet and outlet of the heat exchanger. Reynolds number used here is based on average velocity in the channel and the hydraulic diameter D_h,

$$\mathrm{Re} = \frac{m.D_h}{A.m} \quad ....(9)$$

Where

$$D_h = \frac{4 \times \text{channel cross sectional area}}{\text{wetted perimeter}}$$

The average Nusselt number is

$$Nu = \frac{h.D_h}{k} \quad . \quad .....(10)$$

Where the heat transfer coefficient h founded from:

$$h = \frac{Q_{convection}}{A_{heat}(T_w - T_b)} \quad ....(11)$$

$$Q_{convection} = Q_{total} - Q_{losses} \quad .....(12)$$

Maximum losses occur through threads connections with the PTFE pieces, and Q_{total} represented the power supply

The friction factor is given by the following equation [11]:

$$f = \frac{\Delta P_{HE}}{\frac{r.V^2}{2}}.\frac{D_h}{L} \quad ....(13)$$

In the above equation, L represents the dimension of the channel in the stream wise direction. The value of the ΔP_{HE} is:

$$\Delta P_{HE} = \Delta P_{23} \quad .....(14)$$

The overall thermal performance is defined by [1]:

$$h = \frac{\frac{Nu}{Nu_o}}{\left(\frac{f}{f_o}\right)^{0.3}} \quad ....(15)$$

Where

Nu_o and f_o are the reference Nusselt number and the reference friction factor for case without pins.

The method of estimating uncertainty in experimental results is based on a careful specification of the uncertainties in the various primary experimental measurements [14]. In the current work The uncertainty in each Reynolds number, heat transfer coefficient, Nusselt Number and friction factor where computed [13].

4-Theoretical Analysis

Figure (5a) shows the physical model of the annular pin fin heat exchanger. The theoretical method of analysis must be capable of simulating the complex flow condition particularly in the near pins region. For this purpose the well known Fluent (6.3) package was utilized for solving the governing equations (continuity, momentum and energy) for steady three-dimensional turbulent compressible flow in addition to thermal performance and cooling effectiveness of the annular pin fin heat exchanger exposed to constant heat flux. The main assumptions are:

1-The cooling fluid is a dry air which flows over and around the pins in a compressible steady and three-dimensional flow.

2-The fluid is a Newtonian and the turbulence model is under Boussineqs approach.

3-The momentum field is subjected to no-slip boundary conditions at the wall. The thermo physical properties (C_P, k, μ) of the fluid are functions of temperature [13].

Reynolds averaged Navier-Stokes equations (RANS) with the RNG k-e turbulence model has been adopted for the present work because it provides more performance than standard model, especially in complex shear flow and flows with high strain rates , swirl and separation [11]. The boundary conditions are shown in figure(5b).

In the current study the unstructured tetrahedron meshes (with 1200000 cell) were chosen as shown in figure (5c). The computer used was (1.16 GHz). The time needed was 48 hour for each reading

5-Results and Discussion

Figure (6) shows the Nusselt number as a function of Reynolds number for the annular heat exchanger exposed to constant heat flux. It appears that the heat transfer to the coolant by convection increases with Reynolds number and is always greater for the pin fin heat exchanger than the smooth channel without pins at any given Reynolds number. According to figure (6), the presence of pin fins enhances the heat transfer by a factor of 1.31 to 1.42 over the range of Reynolds number studied 6774 to 11120.

Figure (6) also displays correlation from Incropera and Dewitt [15] valid for turbulent fully developed flow in circular tubes. It appears that the experimental results for smooth channel without pins are in very good agreement with this correlation [15]. This match insures the reliability of the experimental apparatus and validity of all heat transfer experimental data.

Further in figure (6) the pin fins heat exchanger experimental results are compared with the theoretical results obtained from FLUENT code. Reasonable agreement between the two results is obtained with average

difference 5% over the Reynolds numbers range.

The Nusselt-Reynolds power correlation suggested for the pin fin heat exchanger is given by the equation.

$$Nu = 0.0109\,\mathrm{Re}^{0.928}\,\mathrm{Pr}^{0.4} \quad \text{----------16}$$

This equation was obtained from the trend line for least square method shown in figure (9).

Figure (7) shows the experimental friction factor obtained from equation (13). According to the results obtained the presence of pin fins increases the friction factor by 3 to 4 times compared to the one obtained for smooth annular channel without pins over the range of Reynolds number. The correlation from Incropera and Dewitt [15] valid for turbulent fully developed flow in a circular tube is also shown in figure (7). It appears that the experimental results for smooth annulus flow are in good agreement with the results from Incropera and Dewitt [15]. Again this match confirms the validity of the pressure losses experimental data.

The pin fin heat exchanger experimental results are compared with theoretical results obtained from FLUENT code as in figure (7). Reasonable agreement between the two results is appeared.

The overall thermal performance η as defined in equation (15), is given in figure (8) for both the experimental and theoretical results from FLUENT. At high Reynolds number the theoretical thermal performance η is lower than the experimental results. This may be attributed to the shortcoming of the turbulence model to predict the mixing flow which resulted in higher friction factor than the actual value [11,13]. At any Reynolds numbers η is larger than 1 meaning that the pin fin heat exchanger performance always exceeds the smooth annular channel.

Figure (10) to (17) show the cooling air velocity contour for two Reynolds numbers 6774 & 11120 at radius r=11.6, 12, 12.5, and 13.2 mm, respectively. It can be noted for all figures as the flow approaches the first row of pin fins, it accelerates around it and boundary layer flow with separation is observed downstream of pin fins. A pair of counter rotating vortices is formed downstream face of each pin. The main stream flow accelerates in the gap region before impinging on the leading edge on the second row pin fins which are staggered to the first row pin fins. The effect of wake behind the pin decreases due to the increase of velocity between pins.

The blockage due to wake of pins, cause flow chocking which appears as a velocity increase in the stream wise direction. Figures (10) and (13) for Reynolds number 6774, show that there is an increase in velocity toward the outer surface. This is due to the more interaction region the staggered array of pins at the inner surface than outer surface which causes more wake behind pins and this leads to chocked flow. The velocity contour at the other Reynolds number shows a similar behavior but at lower velocity due to properties (density and temperature) effects.

Figures (18) to (21) show the temperature contours on outer cylinder heated surface. All contours show a lower temperature region around the pins in all rows due to the impinging of main stream flow on leading edge. The overall temperature about the outer cylinder heated surface, decreased gradually as shown in figures (18) to (21) with increasing Reynolds number. A mountain shape profile appears across the pins. This may be due to the horse shoe vortices which bring cooler fluid from the core region of the channel towards the channel end wall [16]. In general, the pin fins produced strong turbulent mixing between the coolant in the core region and hotter air near the channel end walls and pin fins.

6-Conclusions

The prominent conclusions of the current study are:

1-The heat transfer to the coolant by convection was always greater for the pin fin heat exchanger than the smooth channel without pins at any given Reynolds number. The pin fins enhanced the heat transfer by a factor of (1.31 to 1.42). The Nusselt-Reynolds correlation obtained from the experimental data was given as:

$$Nu = 0.0109\,\mathrm{Re}^{0.928}\,\mathrm{Pr}^{0.4}$$

2- A reasonable agreement between pin fins heat exchanger experimental results and theoretical results were obtained with average difference (5%) over the Reynolds numbers range.

3- The presence of pin fins increased the friction factor by (3 to 4) times compared to the one obtained from smooth annular channel without pins. A reasonable agreement between the experimental and theoretical friction factors was obtained.

4- At any Reynolds number, the overall thermal performance was larger than (1) meaning that the pin fin heat exchanger performance always exceeded the smooth annular channel.

5- Pin fins were very effective in heat transfer enhancement due to turbulent mixing caused by flow separation around the pin fins and the formation of horse shoe vortices in the junction between the pin fins and the channel wall.

Finally, it may be conclude that the convective cooling scheme like pin fins has the ability to enhance the heat transfer greatly and can be used in the internal cooling applications.

References

[1].Marques, C. "Manufacturing and analysis of a LIGA heat exchanger for the surface of a tube: a cooling simulation of the leading edge region of a turbine blade", Ph.D. Dissertation, Agricultural and Mechanical, Louisiana State University, USA, 2003

[2]. Metzger, DE.: Fan, CS. and Haley, SW. "Effects of pin shape and array orientation on heat transfer and pressure loss in pin fin arrays". ASME J Eng Gas Turbines Power, 1984, Vol.106 pp252–257.

[3]. Metzger, D.E. ; Berry, R.A. and Bronson, J.P., "Developing Heat Transfer in Rectangular Ducts With Staggered Arrays of Short Pin Fins", Journal of Heat Transfer, Vol. 104, Nov 1982, pp. 700-706.

[4]. Chyu, M.K. "Heat Transfer and Pressure Drop for Short Pin-Fin Arrays with Pin- End wall Fillet", Journal of Heat Transfer, Vol. 112, 1990, pp. 926-932.

[5]. Chyu, M.K., ; Yen, C.H., ; Ma, W., and Shih, T. I-P., "Effects of Flow Gap Atop Pin Elements on The Heat Transfer from Pin Fin Arrays", Presented at the International Gas Turbine & Aeroengine Congress & Exhibition, Indianapolis, June 7-10, 1999.

[6]. Uzol, O. and Camci, C. "Elliptical pin fins as an alternative to circular pin fins for gas turbine blade cooling applications. Part 2: wake flow field measurements and visualizations using PIV". Presented at the 46th ASME international gas turbine, aeroengine congress and exposition and users symposium, 2001, New Orleans, LA

[7] Yan, WM. and Sheen, PJ. "Heat transfer and friction characteristics of fin-and-tube heat exchangers". Int J Heat Mass Transfer, 2000, Vol. 43, pp.1651–1659.

[8].Yan, WM.; Li, HY. and Tsay, YL. "Thermo Fluid characteristics of frosted-tube heat exchangers". Int J Heat Mass Transfer, 2005, Vol. 48(15), pp.3073–3080.

[9] Mizunuma, H.; Behnia, M. and Nakayama, W. "Heat transfer from micro-finned surfaces to flow of fluorinert coolant in reduced-size channels". IEEE Trans Components Packaging Manufacturing Technol Part A, 1997, Vol.20(2), pp.139–145.

[10] Marques, C. and Kelly, KW. "Fabrication and performance of a pin fin micro heat exchanger". ASME J. Heat Transfer, 2004, Vol. 126, pp.434–444.

[11] Galvis, E.; B. A. Jubran; Behdinan F. Xi K and Fawaz, Z. "Numerical modeling of pin–fin micro heat exchangers", Journal of Heat Mass Transfer, 2008, vol-44:pp 659–666.

[12. Holman, J.P. *Heat Transfer*, McGraw-Hill, 9th edition, 2008.

[13] Abbo, A.A. "Simulation of Pin Fin Heat Exchanger Used in Turbine Blade" Ph.D. Thesis, Mechanical Engineering Dep. U.O.T, 2009.

[14] Holman, J.P. and Gajda, W.J "*Experimental Methods for Engineers*" Fourth Edition, McGraw-Hill, Book Company, 1984

[15] Incropera, F. P. and DeWitt, D. P. Introduction to Heat Transfer, 3rd Edition, John Wiley & Sons, New York, 1996.

[16].Guoguange, S.u.; Hamn,Ching, Chen and Je-Chin, Han "Computational of flow and Heat Transfer in rotating Rectangular Channels (AR=4:1) With Pin-Fins by a Reynolds stress Turbulence Model", Journal of Heat Transfer, Vol.129 June 2007, pp.685-696

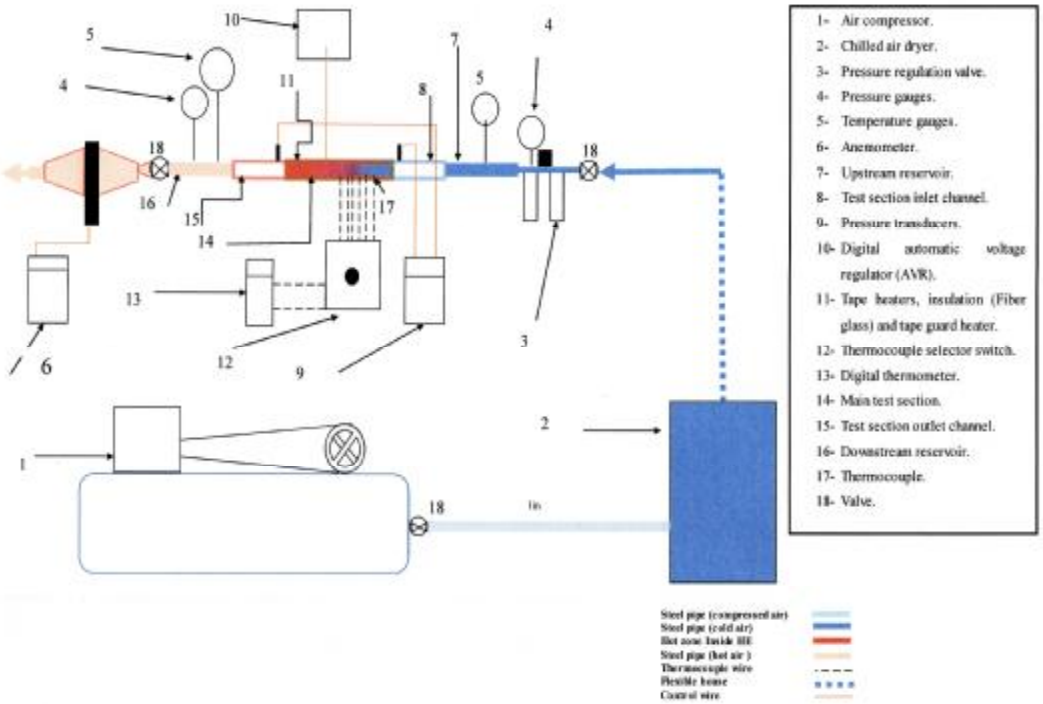

Figure (1) Schematic diagram of the test rig

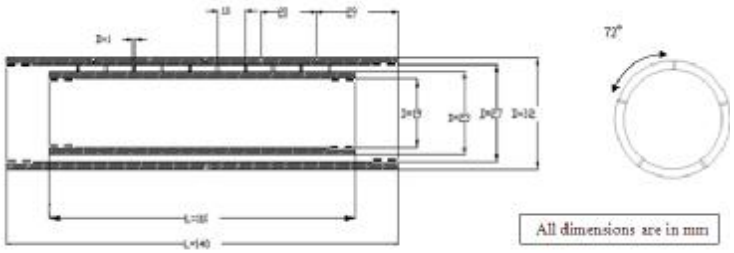

(a) Main test section

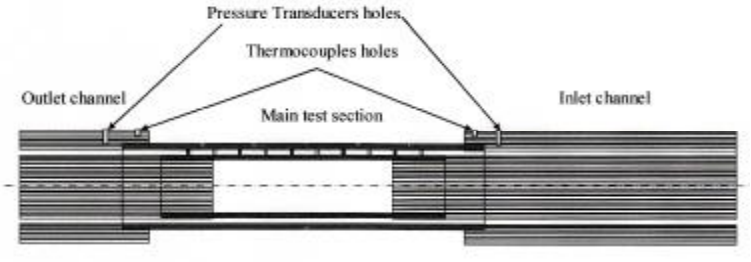

(b) Main test section and inlet and outlet channels assembly

Figure (2) The test section

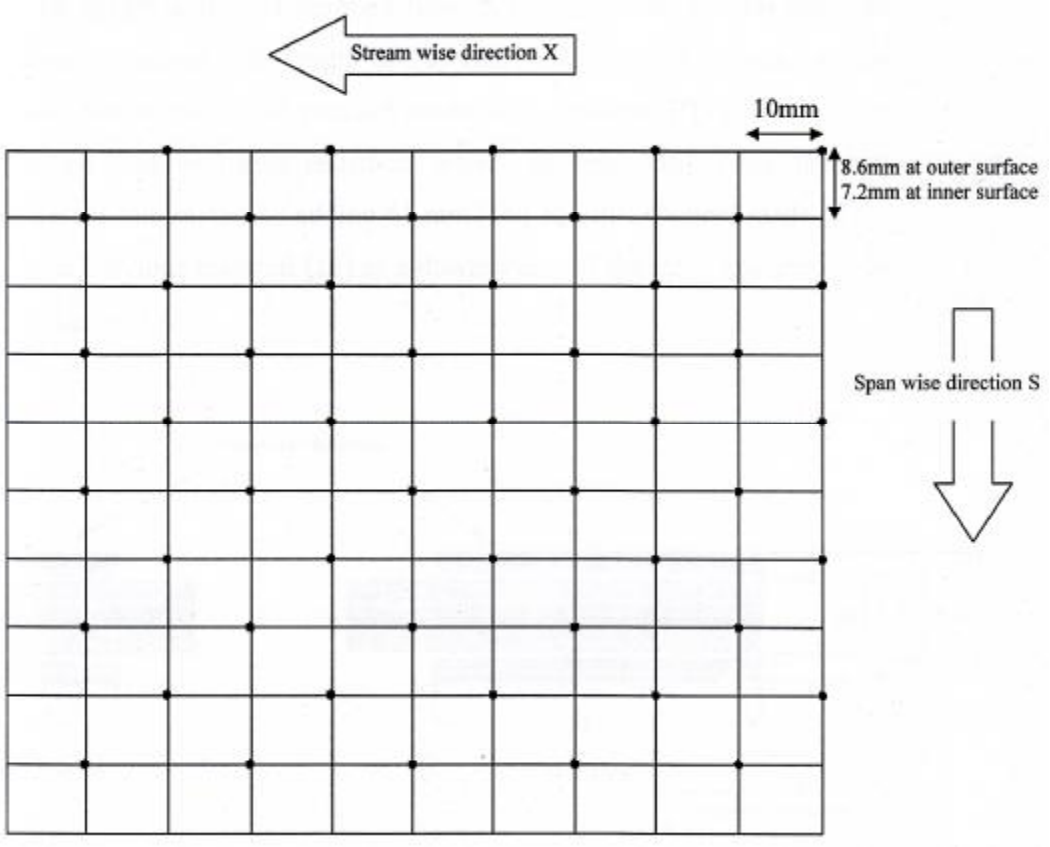

Figure (3) Pin distribution along the channel cylinder surface (staggered)

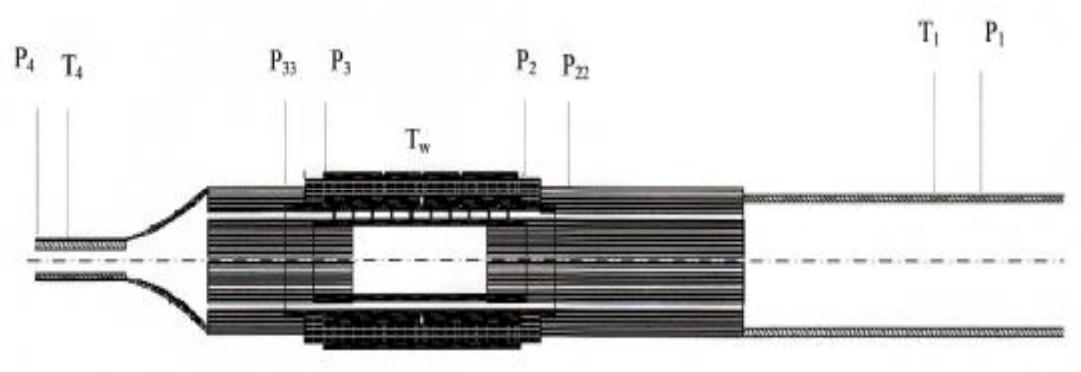

Figure (4) Pressure and Temperature measurement points

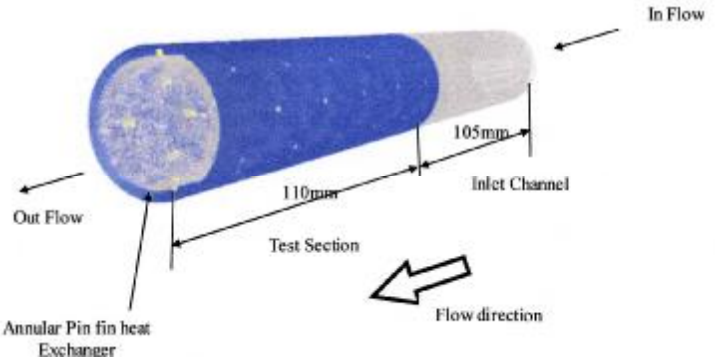

(a) Physical model of the annular pin fin heat exchanger

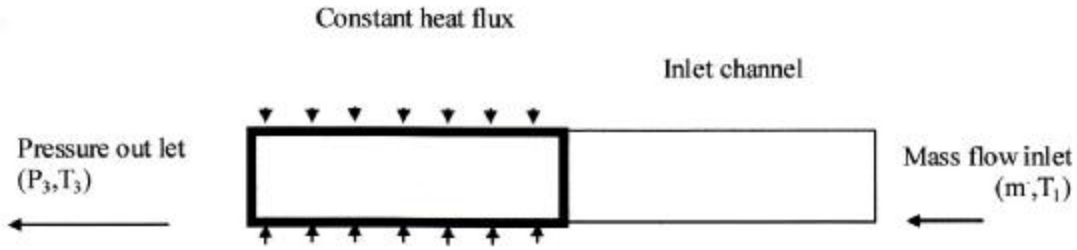

(b) Boundary conditions

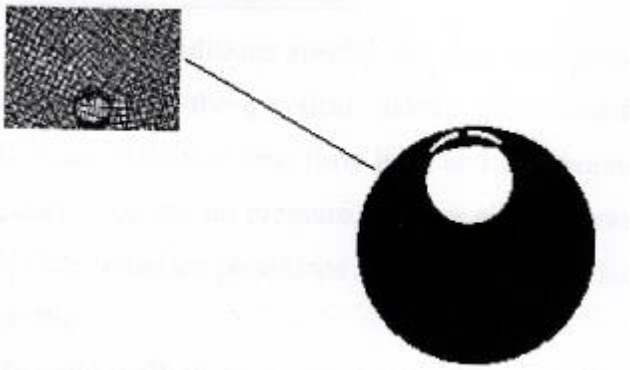

(c) Mesh used in the current study

Figure (5) Physical model, Boundary conditions and the Mesh used in the current study.

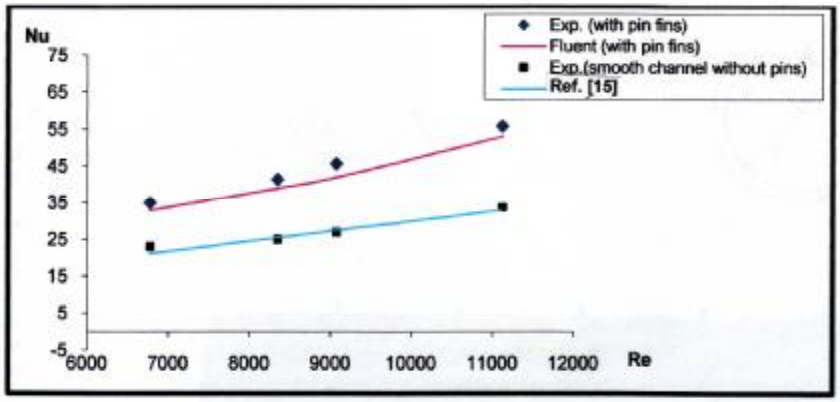

Figure (6) Nusselt number as a function of Reynolds number

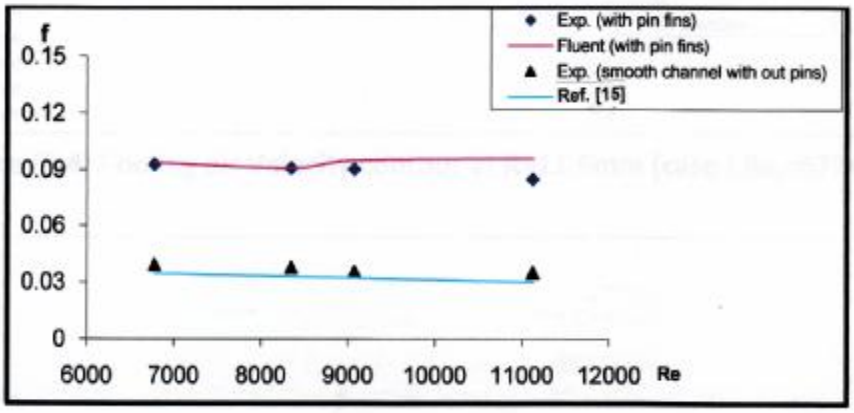

Figure (7) Friction factor as a function of Reynolds number

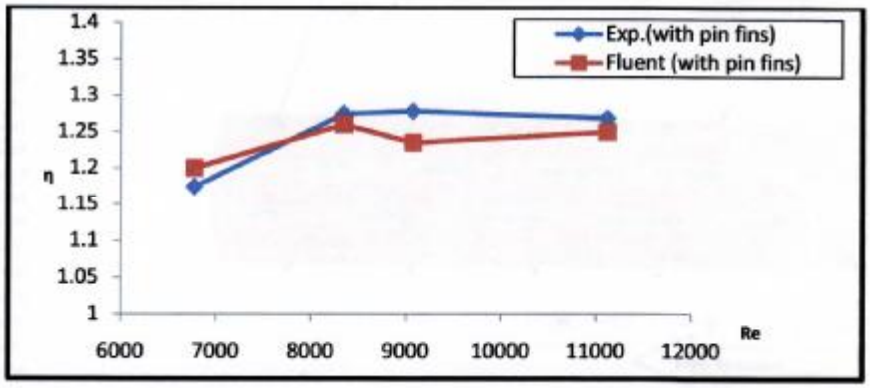

Figure (8) Overall thermal performance as a function of Reynolds number

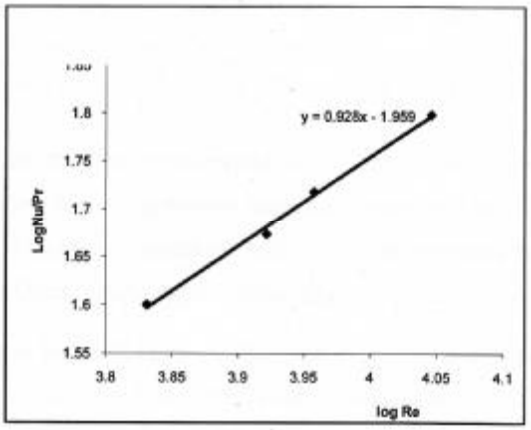

Figure (9) Trend line for least square method

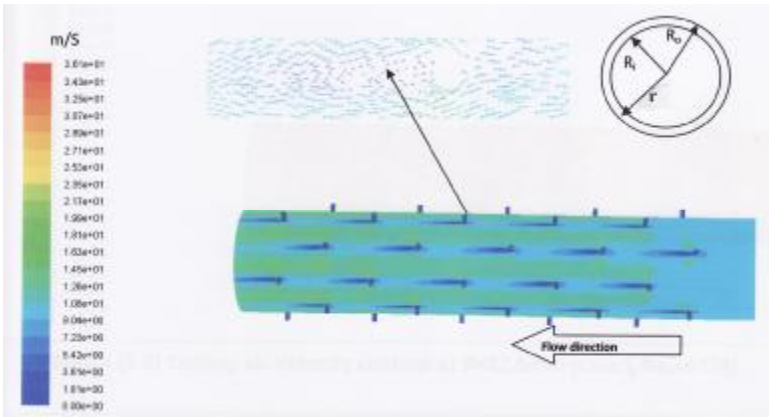

Figure (10) Cooling air Velocity contour at r=11.6mm (Re=6774)

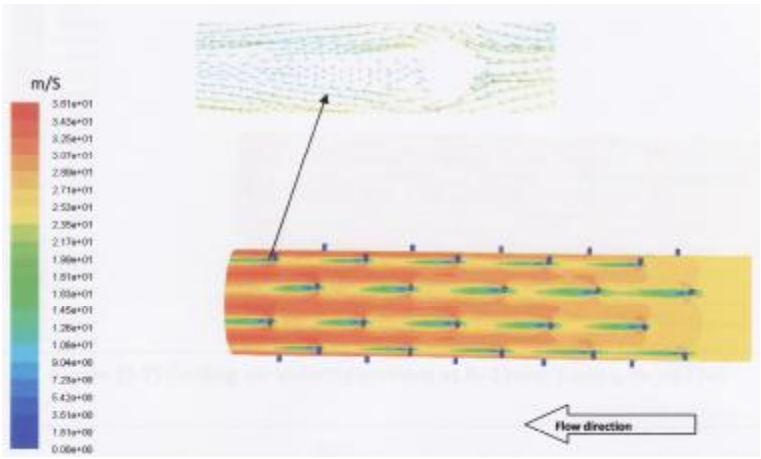

Figure (11) Cooling air Velocity contour at r=12mm (Re=6774)

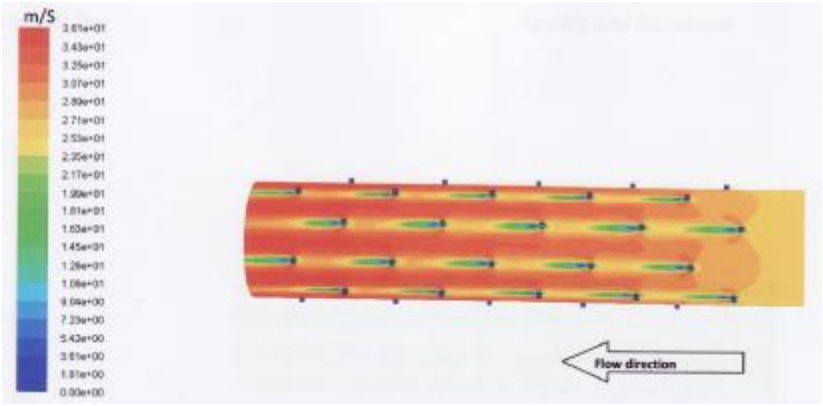

Figure (12) Cooling air Velocity contour at r=12.5mm (Re=6774)

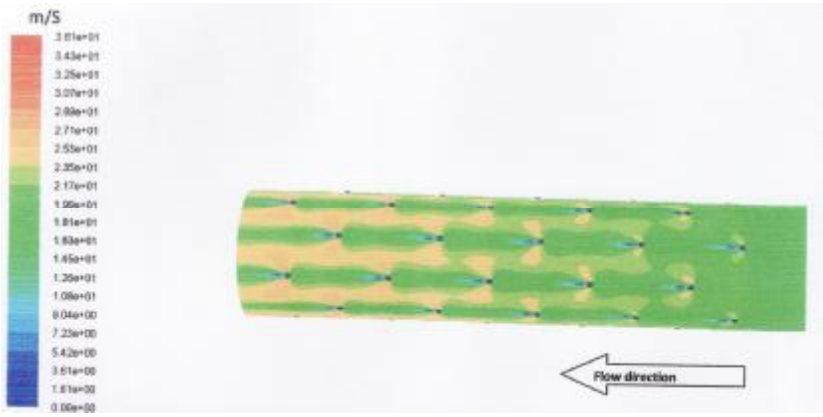

Figure (13) Cooling air Velocity contour at r=13.2mm (Re=6774)

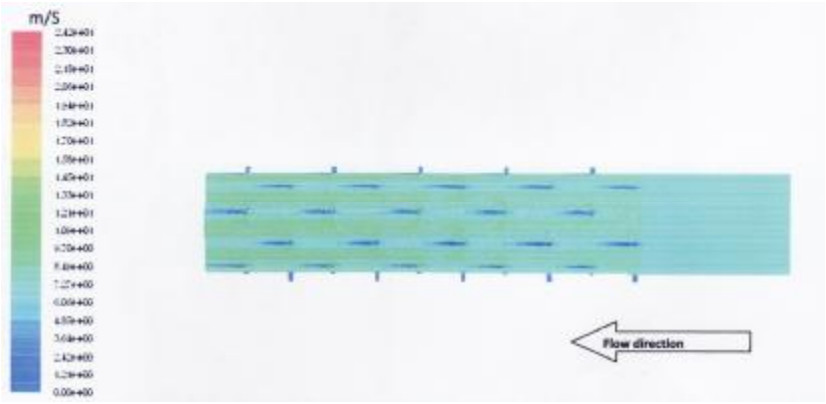

Figure (14) Cooling air Velocity contour at r=11.6mm (Re=11120)

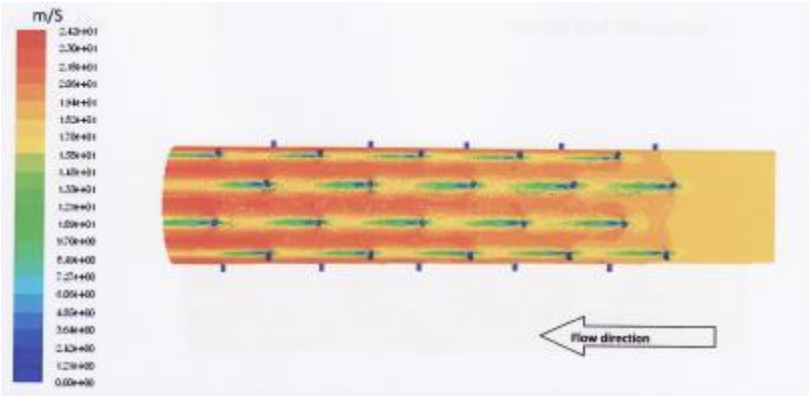

Figure (15) Cooling air Velocity contour at r=12mm (Re=11120)

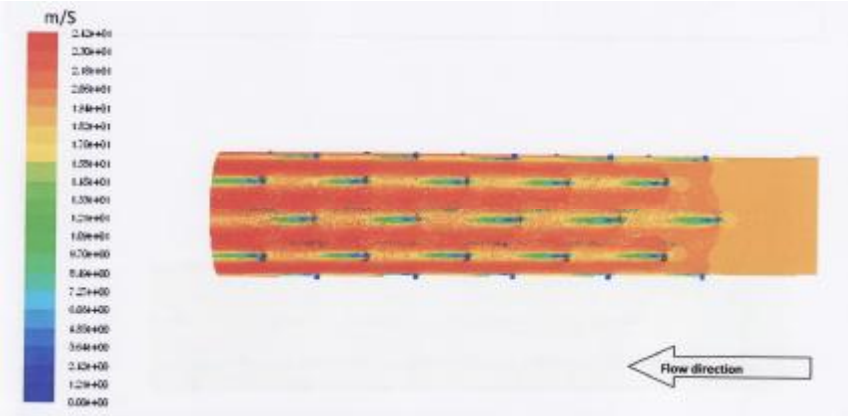

Figure (16) Cooling air Velocity contour at r=12.5mm (Re=11120)

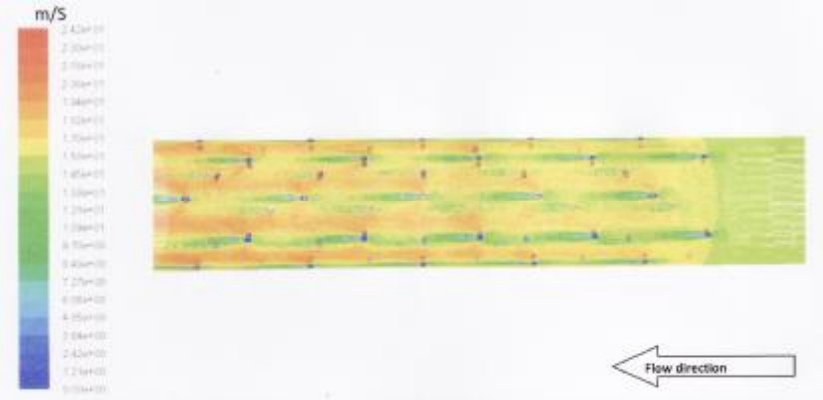

Figure (17) Cooling air Velocity contour at r=13.2mm (Re=11120)

Figure (18) Temperature contour on outer Cylinder heated surface (Re=6774)

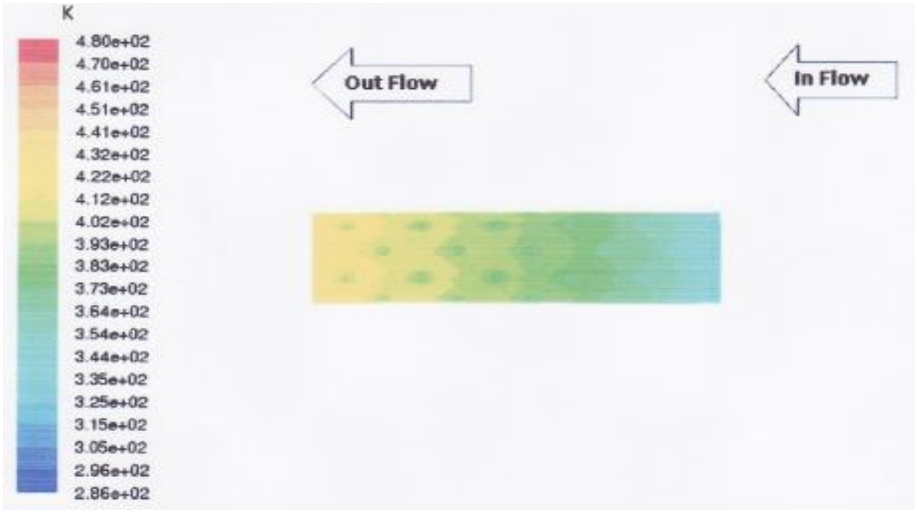

Figure (19) Temperature contour on outer Cylinder heated surface (Re=8346)

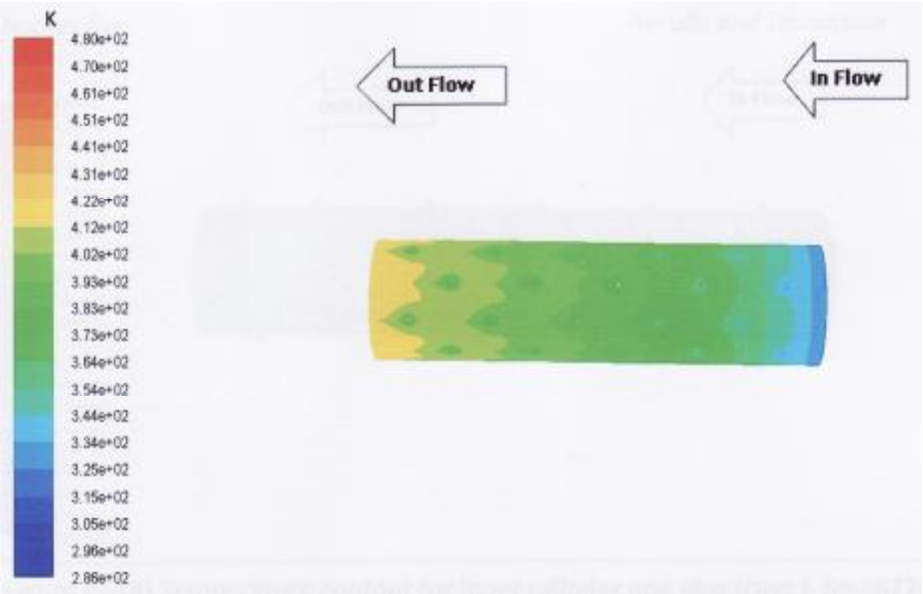

Figure (20) Temperature contour on outer Cylinder heated surface (Re=9072)

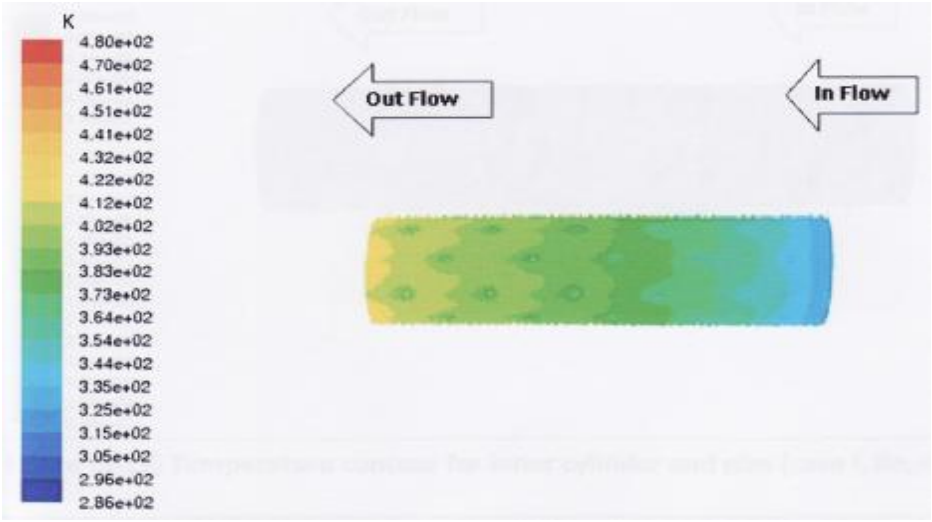

Figure (21) Temperature contour on outer Cylinder heated surface (Re=11120)